

A New Way to Scorpionate Niobium Complexes: Terminal Alkyne, Imido, and Oxo Complexes and the Rearrangement of α -Agostic Ethyl Complexes

Pascal Oulié, Nicolas Bréfuel, Laure Vendier, Carine Duhayon, and Michel Etienne^{*,†}

Laboratoire de Chimie de Coordination du CNRS, UPR 8241, 205 Route de Narbonne, 31077 Toulouse Cedex 04, France

Received May 27, 2005

This paper describes an efficient, straightforward synthesis of new hydrotris(pyrazolyl)borate (Tp') niobium terminal alkyne complexes and some reactions of these complexes. Reduction of the niobium(IV) complexes Tp'NbCl₃ (Tp' = Tp^{Me2} (**1**), Tp^{Me2,4Cl} (**1-Cl**)) with zinc in the presence of a terminal alkyne HC≡CR gives good yields (ca. 75%) of the new alkyne complexes Tp'NbCl₂(HC≡CR) (**2-R**) (R = H, Ph, C₆H₄-4-Me, CH₂Ph, CF₃) and **2-Cl-Ph**. The strategy is significant since the previously reported synthesis of Tp'NbCl₂(RC≡CR') was possible only with *internal* alkynes. NMR data indicate that the four-electron donor alkyne sits in the molecular mirror plane. Restricted alkyne rotation is observed by NMR in solution. The more abundant rotamer has the large substituent located distal to the Tp' ligand, thereby alleviating steric interactions. Only this rotamer is observed in the crystal structures of **2-R** (R = Ph, C₆H₄-4-Me, CH₂Ph). In the crystal structure of **2-CF₃**, however, three independent molecules are observed with both alkyne orientations. The one that has the CF₃ group proximal to Tp^{Me2} exhibits H...F bridges between the alkyne CF₃ group and the methyl group at the 3-position of the Tp^{Me2} ligand. Oxo and imidoniobium complexes are also available via the same synthetic procedure. α -C-H agostic ethyl complexes Tp^{Me2}-NbCl(μ -H-CHCH₃)(HC≡CR) (**4-R**) (R = Ph, C₆H₄-4-Me, CH₂Ph) have been synthesized. Their thermolyses have been studied with the goal of observing the Nb-CH₂CH₃/H-C≡CR exchange leading to the putative Tp^{Me2}NbCl(H)(CH₃CH₂C≡CR). This reaction mainly gives decomposition products, although spectroscopic data suggest that it occurs. This reaction is significant in the context of comparing kinetic and thermodynamic data for M-H versus M-C stability and reactivity.

Introduction

The lack of convenient, simple, easily accessible starting material has been a recurrent problem that has hampered a broad development of the scorpionate or hydro(trispyrazolyl)borate (Tp') chemistry of the heavier group 5 elements Nb and Ta.¹ The synthesis of simple chloro niobium(V) complexes such as TpNbCl₄ and Tp^{Me2}NbCl₄ is highly dependent on experimental conditions, and byproducts formation has precluded the utilization of these complexes as useful starting material.² For tantalum, we recently suggested that Tp^{Me2}-TaCl₂(tht) (tht = tetrahydrothiophene) might be a good candidate, but the unsymmetrical Ta=Ta dimer (Tp^{Me2}-Ta)(TaCl₃)(μ -Cl)₂(μ -tht) that formed in the first step of a proposed reaction sequence was found to be inert toward a second substitution of Tp^{Me2}.³ Instead, the

chemistry developed so far has relied upon the prior introduction of the desired functional group followed by subsequent addition of the Tp' ligand. In this vein, Tp^{Me2}TaMe₃Cl,⁴ Tp^{Me2}MCl₂(RC≡CR') (M = Nb, Ta),^{5,6} Tp^{Me2}Ta(=CH-*t*-Bu)Cl₂,⁷ and Tp^{Me2}M(=NR)Cl₂⁸ have been obtained from TaMe₃Cl₂, MCl₃(dme)(RC≡CR') (dme = 1,2-dimethoxyethane), Ta(=CH-*t*-Bu)Cl₂(thf)₂, and M(=NR)Cl₃L₂ (L = thf, pyridine), respectively. Some of these reactions suffer from occasional drawbacks however. For example, our one-pot synthesis of Tp^{Me2}NbCl₂(RC≡CR') is possible only in the case of *internal* alkynes since it uses [NbCl₃(dme)]_n as the niobium source, a compound that catalytically trimerizes *terminal* alkynes.⁹ More recently,¹⁰ the synthesis

[†] E-mail: etienne@cc-toulouse.fr.

(1) (a) *Scorpionates - The Coordination Chemistry of Polypyrazolylborate Ligands*; Trofimenko, S., Ed.; Imperial College Press: London, 1999. (b) Etienne, M. *Coord. Chem. Rev.* **1996**, *156*, 201–236. (c) We will use throughout the nomenclature proposed by S. Trofimenko; see ref 1a.

(2) (a) Hubert-Pflazgraf, L.; Tsunoda, M. *Polyhedron* **1983**, *2*, 203–210. (b) Bradley, D. C.; Hursthouse, M. B.; Newton, J.; Walker, N. P. *C. J. Chem. Soc., Chem. Commun.* **1984**, 188–190.

(3) Etienne, M.; Hierso, J.-C.; Daff, P. J.; Donnadiou, B.; Dahan, F. *Polyhedron* **2004**, *23*, 379–383.

(4) Reger, D. L.; Swift, C. A.; Lebioda, L. *Inorg. Chem.* **1984**, *23*, 349–354.

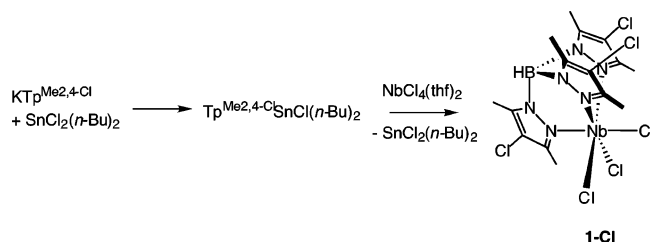
(5) Etienne, M.; Biasotto, F.; Mathieu, R.; Templeton, J. L. *Organometallics* **1996**, *15*, 1106–1112.

(6) Hierso, J.-C.; Etienne, M. *Eur. J. Inorg. Chem.* **2000**, 839–842.

(7) Boncella, J. M.; Cajigal, M. L.; Abboud, K. A. *Organometallics* **1996**, *15*, 1905–1912.

(8) (a) Sundermeyer, J.; Putterlik, J.; Foth, M.; Field, J. S.; Ramesar, N. *Chem. Ber.* **1994**, *127*, 1201–1212. (b) Boncella, J. M.; Cajigal, M. L.; Gamble, A. S.; Abboud, K. A. *Polyhedron* **1996**, *15*, 2071–2078 (c) Weber, K.; Klorn, K.; Schorm, A.; Kipke, J.; Lemke, M.; Khvorost, A.; Harms, K.; Sundermeyer, J. *Z. Anorg. Allg. Chem.* **2003**, *629*, 744–754 (d) Schorm, A.; Sundermeyer, J. *Eur. J. Inorg. Chem.* **2001**, 2947–2955.

Scheme 1



of the niobium(IV) complex $\text{Tp}^{\text{Me}2}\text{NbCl}_3$ (**1**) from $\text{NbCl}_4(\text{thf})_2$ and $\text{Tp}^{\text{Me}2}\text{SnClBu}_2$ has been described. Both the synthesis of the tin reagent¹¹ and that of **1** seemed straightforward, and **1** thus appeared to be the long sought simple starting material in $\text{Tp}'\text{Nb}$ chemistry. Indeed we report herein that this compound can be readily reduced to give (i) known internal alkyne complexes $\text{Tp}'\text{NbCl}_2(\text{RC}\equiv\text{CR}')$ ($\text{Tp}' = \text{Tp}^{\text{Me}2}, \text{Tp}^{\text{Me}2,4\text{Cl}}$), (ii) more significantly, previously unknown *terminal* alkyne complexes $\text{Tp}'\text{NbCl}_2(\text{HC}\equiv\text{CR})$, and (iii) oxo and imido complexes based on $\text{Tp}'\text{Nb}$. Some reactivity of $\text{Tp}'\text{NbCl}_2(\text{HC}\equiv\text{CR})$, aimed at probing the migratory aptitudes of alkyl versus hydride to a coordinated alkyne, is also described.

Results and Discussion

New Tp' Complexes Based on $\text{Tp}'\text{NbCl}_3$. Reaction of the tin compounds $\text{Tp}^{\text{Me}2}\text{SnClBu}_2$ and $\text{Tp}^{\text{Me}2,4\text{Cl}}\text{SnClBu}_2$ with $\text{NbCl}_4(\text{thf})_2$ results in the formation of $\text{Tp}^{\text{Me}2}\text{NbCl}_3$ (**1**) and $\text{Tp}^{\text{Me}2,4\text{Cl}}\text{NbCl}_3$ (**1-Cl**), respectively (Scheme 1).¹² In the initial report,^{10a} the yield of **1** was limited without obvious reasons to 41% and scale-up was desirable. We have found that carrying out the reaction between either of the tin complexes with $\text{NbCl}_4(\text{thf})_2$ first in toluene (as a slurry) for 4 days in the dark and then, after evaporating the toluene, for 2 days in dichloromethane yielded **1** or the new **1-Cl** in 78% yield on a 10 mmol scale or more. **1-Cl** is obtained as bright golden yellow microcrystals indefinitely stable under dinitrogen. Both compounds exhibit similar X-band ESR parameters (for **1**, dichloromethane, 293 K, $g = 1.93$, $A_{\text{iso}} = 170$ G (10 lines); dichloromethane/toluene, 100 K, $g_1 = 1.91$, $g_2 = 1.94$, $g_3 = 1.92$, $A_1 = 258$, $A_2 = 123$, $A_3 = 126$ G) in agreement with an almost perfect C_{3v} symmetry.

As a first probe of the potential use of **1** and **1-Cl** in synthesis, we checked that a representative complex in the series, namely, $\text{Tp}^{\text{Me}2}\text{NbCl}_2(\text{PhC}\equiv\text{CMe})$,⁵ could be obtained. Reduction of **1** with excess zinc in thf in the presence of $\text{PhC}\equiv\text{CMe}$ indeed yields the known $\text{Tp}^{\text{Me}2}\text{NbCl}_2(\text{PhC}\equiv\text{CMe})$ in more than 75% yield after workup. Following the same procedure, reaction of **1** or **1-Cl** with terminal alkynes $\text{HC}\equiv\text{CR}$ with a variety of substituents ($\text{R} = \text{H}, \text{Ph}, \text{C}_6\text{H}_4\text{-4-Me}, \text{CH}_2\text{Ph}, \text{CF}_3$) proceeds smoothly to give $\text{Tp}'\text{NbCl}_2(\text{HC}\equiv\text{CR})$ **2-R** and **2-Cl-R** in equally

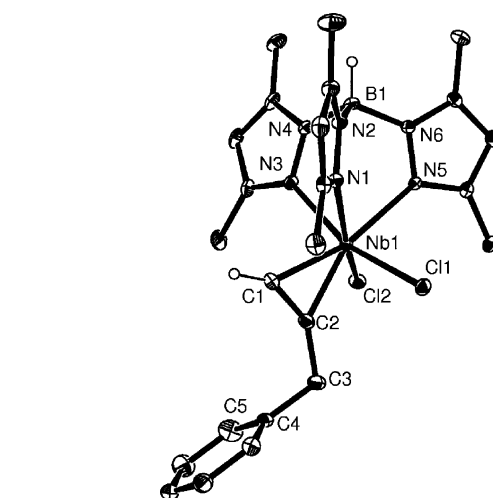


Figure 1. Plot of the molecular structure of $\text{Tp}^{\text{Me}2}\text{NbCl}_2(\text{HC}\equiv\text{CCH}_2\text{Ph})$, **2-CH}_2\text{Ph}**.

Scheme 2

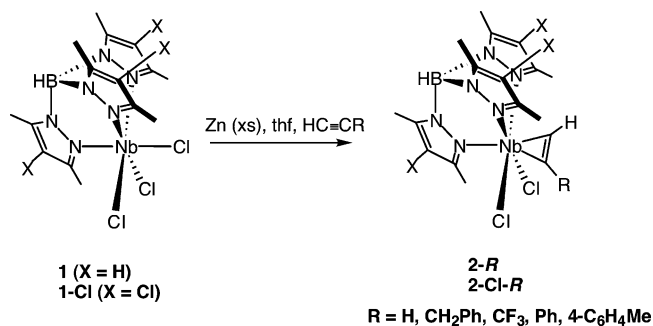


Table 1. Selected Bond Lengths and Angles for $\text{Tp}^{\text{Me}2}\text{NbCl}_2(\text{HC}\equiv\text{CCH}_2\text{Ph})$ (**2-CH}_2\text{Ph}**)

Bond Lengths (Å)	
Nb(1)–Cl(1)	2.4039(5)
Nb(1)–Cl(2)	2.4079(5)
Nb(1)–C(1)	2.0797(19)
Nb(1)–C(2)	2.0686(18)
C(1)–C(2)	1.297(3)
Bond Angles (deg)	
Cl(1)–Nb(1)–Cl(2)	105.07(2)
C(1)–C(2)–C(3)	147.60(19)
C(1)–Nb(1)–C(2)	36.43(8)

good yields according to Scheme 2. No trace of cyclo-trimerization products was observed in the ^1H NMR spectra of crude reaction mixtures. In the case of acetylene itself, some $[\text{Tp}^{\text{Me}2}\text{Nb}(\text{O})\text{Cl}](\mu\text{-O})$ ¹³ was formed along with **2-H**. The formation of this oxo dimer is presumably due to failure to completely remove traces of dioxygen/water present during the generation of acetylene from $\text{NaC}\equiv\text{CH}$ and H_2O . All complexes are purple microcrystalline solids that have been fully characterized by elemental analysis, ^1H and ^{13}C NMR spectroscopy, and, in two cases, X-ray diffraction.

Prominent metric parameters and an ORTEP plot for $\text{Tp}^{\text{Me}2}\text{NbCl}_2(\text{HC}\equiv\text{CCH}_2\text{Ph})$ **2-CH}_2\text{Ph}** are collected in Table 1 and Figure 1, respectively. The alkyne sits in the molecular symmetry plane, and the terminal C–H is proximal to the $\text{Tp}^{\text{Me}2}$. This conformation directs the benzyl moiety away from the pendant Me groups of

(9) (a) Roskamp, E. J.; Pedersen, S. F. *J. Am. Chem. Soc.* **1987**, *109*, 3170–3172. (b) Hartung, J. B.; Pedersen, S. F. *Organometallics* **1990**, *9*, 1414–1417.

(10) (a) Mashima, K.; Oshiki, T.; Tani, K. *Organometallics* **1997**, *16*, 2760–2762. (b) Oshiki, T.; Mashima, K.; Kawamura, S.; Tani, K.; Kitauro, K. *Bull. Chem. Soc. Jpn.* **2000**, *73*, 1735–1748.

(11) Lobbia, G. F.; Bonati, F.; Cecchi, P.; Lorenzotti, A.; Pettinari, C. *J. Organomet. Chem.* **1991**, *403*, 317–323.

(12) $\text{Tp}^{\text{Me}2,4\text{Cl}}\text{SnClBu}_2$ is a new compound obtained and characterized in the same way as related complexes; see: Lobbia, G. F.; Cecchi, P.; Calogero, S.; Valle, G.; Chiarini, M.; Stievano, L. *J. Organomet. Chem.* **1995**, *503*, 297–305.

(13) Antinolo, A.; Carrillo-Hermosilla, F.; Fernandez-Baeza, J.; Lanfranchi, M.; Lara-Sanchez, A.; Otero, A.; Palomares, E.; Pellinghelli, M. A.; Rodriguez, A. M. *Organometallics* **1998**, *17*, 3015–3019.

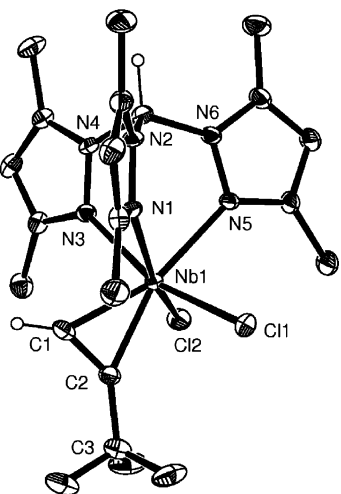


Figure 2. Plot of one independent molecule of $\text{Tp}^{\text{Me}_2}\text{NbCl}_2(\text{HC}\equiv\text{CCF}_3)$, **2-CF₃**.

Tp^{Me_2} . Short Nb–C bonds (average 2.073 Å) between the Nb center and the coordinated alkyne, as well as a bent back angle C(1)–C(2)–C(3) of 147.6(2)°, are indicative of the four-electron donor behavior of the alkyne ligand.¹⁵ This situation is akin to that of the phenylpropyne complex $\text{Tp}^{\text{Me}_2}\text{NbCl}_2(\text{PhC}\equiv\text{CMe})$:¹⁴ the whole alkyne including the phenyl ring lies in the molecular symmetry plane, and the phenyl group is proximal to the Tp^{Me_2} ligand. In the X-ray crystal structures of **2-Ph** and **2-C₆H₄-4-Me** the same overall geometry is observed: the whole alkyne with its phenyl group is in the molecular mirror plane, the phenyl group being distal to Tp^{Me_2} as in **2-CH₂Ph**. Disorder problems have precluded a detailed discussion of the bonding parameters for these complexes. Accordingly, the bonding picture in these formally niobium(III) alkyne complexes is also consistent with a reduced alkyne and an oxidized niobium(V) center, i.e., a metallacyclopentadiene description. Related cyclopentadienyl¹⁶ and six-coordinate^{9b,17} niobium complexes exhibit similar bonding features.

Perhaps more surprising is the X-ray crystal structure of $\text{Tp}^{\text{Me}_2}\text{NbCl}_2(\text{HC}\equiv\text{CCF}_3)$ (**2-CF₃**). The asymmetric unit now contains three independent molecules. Interestingly, they exhibit different alkyne orientations. For two of them, the overall alkyne orientation is similar to that for **2-CH₂Ph**. The trifluoromethyl group is oriented toward the two *cis* chloro ligands, directing the CH between the two *cis* pyrazolyl rings. One of the molecules is highly symmetrical (Figure 2, Table 2). The whole alkyne including one fluorine of the trifluoromethyl group lies virtually perfectly in the molecular symmetry plane. In the other one, there are slight differences in the dihedral angles defining the precise alkyne orientation with respect to the $\text{Tp}^{\text{Me}_2}\text{NbCl}_2$ moiety, and the pyrazolyl ring *trans* to the alkyne is slightly distorted. Also the conformation of the trifluoromethyl group is different. There are some significant differences in the Nb–alkyne metric parameters. One of the two molecules exhibits a more symmetrical Nb–alkyne bonding;

Table 2. Selected Bond Lengths and Angles for $\text{Tp}^{\text{Me}_2}\text{NbCl}_2(\text{HC}\equiv\text{CCF}_3)$ (2-CF₃**)^a**

Bond Lengths (Å)	
Nb(1)–Cl(1)	2.3775(12)
Nb(1)–Cl(2)	2.3760(15)
Nb(1)–C(1)	2.101(5)
Nb(1)–C(2)	2.073(5)
C(1)–C(2)	1.303(8)
Bond Angles (deg)	
Cl(1)–Nb(1)–Cl(2)	104.19(5)
C(1)–Nb(1)–C(2)	36.4(2)
C(1)–C(2)–C(3)	140.5(5)

^a Data for one of the three independent complexes, with the same alkyne orientation as that in **2-CH₂Ph**; see Figure 2. Metric parameters for the two others do not differ significantly; see text.

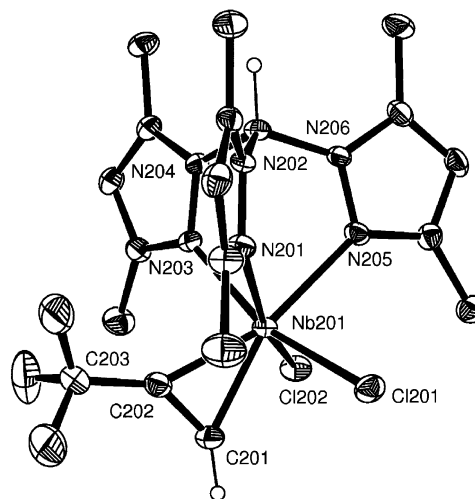


Figure 3. Plot of one independent molecule of $\text{Tp}^{\text{Me}_2}\text{NbCl}_2(\text{HC}\equiv\text{CCF}_3)$, **2-CF₃**, with a different alkyne orientation.

namely, Nb–CH distances are 2.101(5) and 2.171(5) Å, and Nb–CCF₃ are 2.073(5) and 2.058(6) Å, respectively, whereas corresponding alkyne C–C distances are 1.303(8) and 1.331(8) Å. There are also small variations of the angles defining the geometry of the overall Nb(HC≡CCF₃) bonding.

For the third independent molecule (Figure 3), the alkyne is rotated approximately by 180° so that the trifluoromethyl group is now directed toward the *cis* pyrazolyl groups. Again, metric parameters characteristic of (4e)-alkyne bonding are observed. They are virtually identical to that for the molecule showing the more symmetrical Nb–alkyne bonding in the aforementioned orientation. This highly original situation where two rotamers of an alkyne are observed in the same crystal is the result of competing effects of comparable magnitudes. The most ubiquitous effects are restricted alkyne rotation arising from steric and orbital effects of similar energies for the two rotamers (see below for a study in solution) and crystal packing, as for **2-CH₂Ph** and related complexes. In the case of **2-CF₃** in addition, there are short intramolecular H···F contacts (between 2.3 and 2.8 Å, when the corresponding C···F contacts are in the 3.2–3.8 Å range)¹⁸ between the trifluoromethyl fluorines and some of the pyrazole 3-CH₃ hydrogens (the sum of van der Waals radii for H and F is 2.67 Å).¹⁹ These distances have been obtained from calculated hydrogen positions, although some hydrogens were located by Fourier differences, in which cases the

(14) Etienne, M.; White, P. S.; Templeton, J. L. *Organometallics* **1991**, *10*, 3801–3803.

(15) Templeton, J. L. *Adv. Organomet. Chem.* **1989**, *29*, 1–100.

(16) (a) Galindo, A.; Gomez, M.; Gomez-Sal, P.; Martin, A.; del Rio, D.; Sanchez, F. *Organometallics* **2002**, *21*, 293–304. (b) Curtis, M. D.; Real, J.; Kwon, D. *Organometallics* **1989**, *8*, 1644–1651.

(17) Cotton, F. A.; Shang, M. *Inorg. Chem.* **1990**, *29*, 508–514.

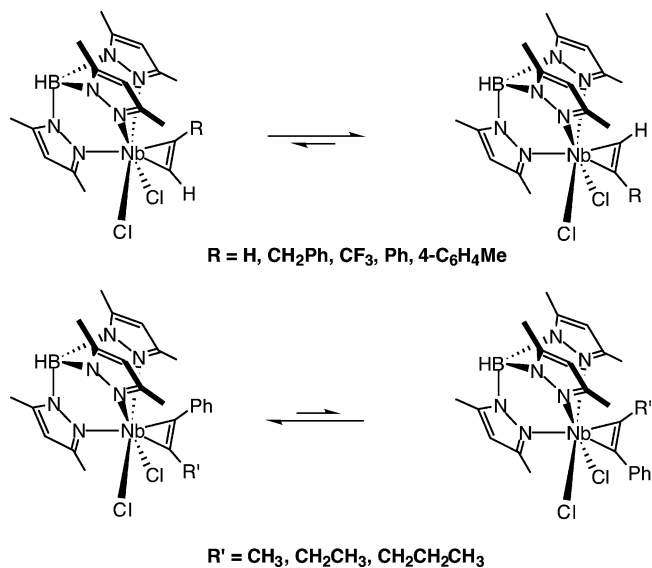
Table 3. Thermodynamic and Kinetic Parameters for the Alkyne Rotation in $\text{Tp}^{\text{Me}_2}\text{NbCl}_2(\text{alkyne})$

alkyne	K° ^a	$\Delta G^\ddagger (T_{\text{coal}}/K)/\text{kJ}\cdot\text{mol}^{-1}$ ^b	ref
HC≡CH		36 (200)	this work
HC≡CCH ₂ Ph	47	62, 53 (293) ^c	this work
HC≡CCF ₃	3.5	52 (293)	this work
HC≡CPh	3	63 (353)	this work
HC≡CC ₆ H ₄ -4-Me	1.6	66 (353)	this work
MeC≡CMe		68 (358)	<i>d</i>
PhC≡CMe	0.17	>80 (>373)	<i>d</i>
PhC≡CCH ₂ Me	0.11	>80 (>373)	<i>d</i>
PhC≡CCH ₂ CH ₂ Me	0.067	>80 (>373)	<i>d</i>

^a Toluene-*d*₈, determined by integration in the ¹H NMR spectra in the slowest exchange limit; see Scheme 3 for details. ^b Determined at T_{coal} of alkyne CH or CCH₃ NMR signals. ^c Shanan-Atidi, H.; Bar-Eli, K. H. *J. Phys. Chem.* **1970**, *74*, 961–963. ^d See ref 5.

distances are of similar magnitude. Even if such interactions are so-called weak interactions or hydrogen bridges,¹⁸ and are therefore not genuine C–F⋯H–C hydrogen bonds, their numbers undoubtedly contribute to the overall alkyne orientation in the case of the somewhat small, unhindered CF₃ group. Several *intermolecular* H⋯F contacts contribute to similar interactions within the asymmetric unit but also to an intricate network within the whole crystal. Recall that in the crystal of $\text{Tp}^{\text{Me}_2}\text{NbCl}_2(\text{PhC}\equiv\text{CMe})$ and related complexes,¹⁴ the phenyl is proximal to Tp^{Me_2} and lies in the molecular symmetry plane, suggesting that π – π or CH– π interactions with the pyrazole rings might be present in addition to steric effects.²⁰ There are thus numerous interactions at play in these systems, but the occurrence of H⋯F interactions leading to a mixture of alkyne rotamers in the solid state of **2-CF₃** was unexpected and is clearly the highlight of this solid state structure.

In the ¹H NMR spectra of **2-R** and **2-Cl-R**, 2:1 and 6:3 intensity patterns for the 4-*H* (in the **2-R** series) and 3- and 5-*Me* pyrazole protons, respectively, indicate that the alkyne sits in the molecular mirror plane. Except for the ethyne complex **2-H**, two sets of such patterns are observed depending on the alkyne orientation with respect to the Tp' ligand, hence on the alkyne rotation barrier (see below). The terminal $\equiv\text{C}-\text{H}$ are characterized by low-field resonances in the range δ 11–14. In the ¹³C NMR spectra, the alkyne carbons bound to Nb also resonate at low field, δ 215–250. The methine carbons appear as doublets with ¹ $J_{\text{CH}} \approx 200$ Hz. These chemical shifts and coupling constants are characteristic of (4e)-alkyne coordination.¹⁵ Restricted alkyne rotation is apparent from the ¹H NMR spectra of all of these complexes. In most cases, coalescence of the alkyne *CH* occurs around room temperature except for **2-H** itself, where coalescence is observed at 200 K ($\Delta\delta = 1.7$ ppm at 173 K, 400 MHz, $\Delta G^\ddagger_{200} = 36$ kJ·mol⁻¹). Thermodynamic and kinetic data for terminal alkyne rotation are summarized in Table 3. They are compared with those for $\text{PhC}\equiv\text{CR}$ (R = Me, CH₂Me, CH₂CH₂Me).¹⁴ The

Scheme 3

equilibrium constant is related to the orientation of the phenyl (or aryl) group with respect to Tp' according to Scheme 3. For $\text{PhC}\equiv\text{CR}$ (R \neq H) complexes, the more populated alkyne rotamer is that with the phenyl ring oriented proximal to Tp^{Me_2} , and as the size of R decreases from CH₂CH₂Me to CH₂Me then to Me, the difference in population decreases. Moving to the smallest substituent, i.e., H in HC≡CPh or HC≡CC₆H₄-4-Me, the same trend is observed, but now the more stable alkyne orientation is observed for the phenyl group sitting away from Tp^{Me_2} . However, for terminal alkyne complexes, the more abundant rotamer is that with the terminal HC≡ oriented proximal to Tp^{Me_2} , a situation also found in the X-ray crystal structure where only this rotamer is observed for **2-CH₂Ph**. For both **2-CH₂Ph** and **2-CF₃**, NOE experiments have confirmed this orientation for the major rotamer. The same situation prevails also in the case of aryl alkyne complexes **2-Ph** and **2-C₆H₄-4-Me**. These equilibria between rotamers are a delicate balance between electronic and steric effects. In the $\text{PhC}\equiv\text{CR}$ complexes, at the lowest temperatures attainable in toluene-*d*₈ or dichloromethane-*d*₂, the phenyl protons always exhibit a 1:2:2 intensity pattern. In the X-ray of $\text{Tp}^{\text{Me}_2}\text{NbCl}_2(\text{PhC}\equiv\text{CMe})$ and related complexes, the phenyl proximal to Tp^{Me_2} lies in the molecular symmetry plane, and this conformation is that adopted in the most abundant rotamer.

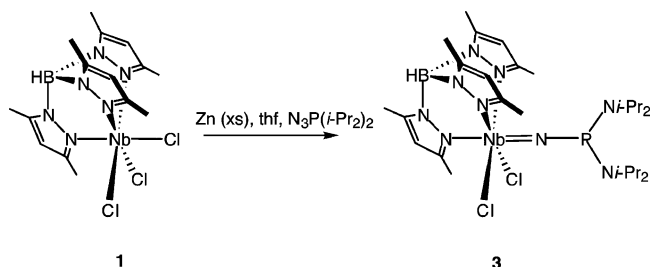
It is not obvious to reconcile solid state and solution data. For the new terminal alkyne complexes, K° increases in the order **2-C₆H₄-4-Me** < **2-Ph** \approx **2-CF₃** \ll **2-CH₂Ph**. This trend does not directly follow the steric hindrance of the substituents, which may be in the order CF₃ < Ph \approx 4-C₆H₄Me < CH₂Ph. Then if attractive H⋯F interactions are operative in solution for **2-CF₃**, they should contribute to a decrease in K° . Note that we have no spectroscopic evidence such as H⋯F or C⋯F through-space couplings, confirming the weakness of these H⋯F interactions.^{18d} One reason for this discrepancy might be that phenyl groups stay in the symmetry plane of the complex as observed in the X-ray of $\text{Tp}^{\text{Me}_2}\text{NbCl}_2(\text{PhC}\equiv\text{CMe})$ and for **2-C₆H₄-4-Me** and **2-Ph**, thereby alleviating unfavorable steric interactions. Also, steric

(18) (a) Hyla-Kryspin, I.; Haufe, G.; Grimme, S. *Chem. Eur. J.* **2004**, *10*, 3411–3422 (b) Desiraju, G. R. *Acc. Chem. Res.* **2002**, *35*, 565–573 (c) Dunitz, J. D.; Taylor, R. *Chem. Eur. J.* **1997**, *3*, 89–98 (d) Mele, A.; Vergani, B.; Viani, F.; Meille, S. V.; Farina, A.; Bravo, P. *Eur. J. Org. Chem.* **1999**, 187, 7–196.

(19) Bondi, A. *J. Phys. Chem.* **1964**, *68*, 441–451.

(20) (a) Hunter, C. A.; Lawson, K. R.; Perkins, J.; Urch, C. J. *J. Chem. Soc., Perkin Trans. 2* **2001**, 651–669. (b) Janiak, C. *J. Chem. Soc., Dalton Trans.* **2000**, 3885–3896.

Scheme 4

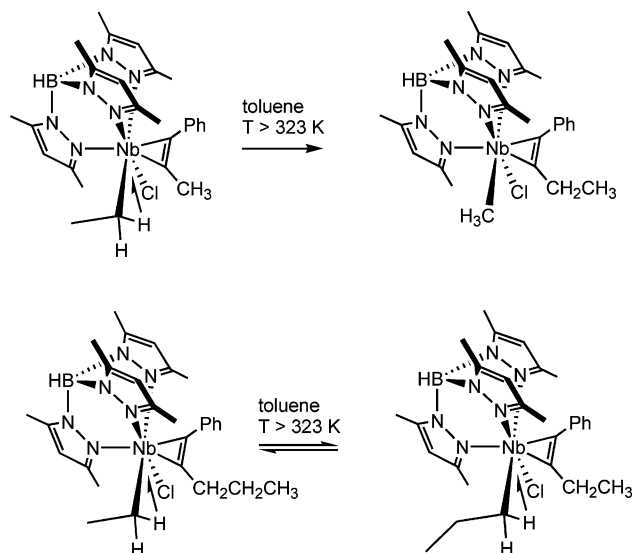


interactions contribute to the barrier to alkyne rotation, but for **2-CF₃** the barrier is slightly smaller than for the other terminal alkyne complexes. It could be argued that attractive H...F interactions should increase the barrier by lowering the ground state. Overall, the barriers for terminal alkynes are similar to that for the 2-butyne complex but notably higher than that for acetylene itself.

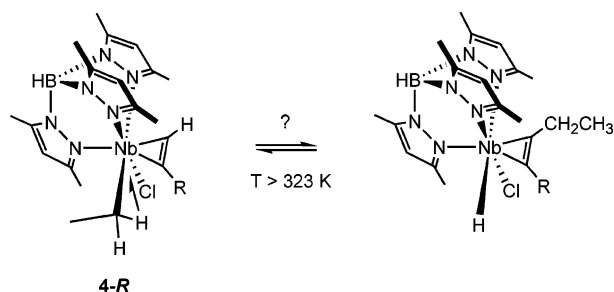
The same reducing conditions used for the syntheses of the terminal alkyne complexes are also efficient for the synthesis of imido complexes. Reaction of **1** with N₃-P(*i*-Pr)₂ and Zn gives the phosphinoimido complex Tp^{Me2}NbCl₂[=N-P(*i*-Pr)₂]**3** in 30% yield (Scheme 4). The molecular symmetry plane in **3** is evidenced by the 2:1 patterns for the pyrazolyl proton and carbon resonances in its ¹H and ¹³C NMR spectra, respectively. The =N-P(*i*-Pr)₂ moiety exhibits a phosphorus resonance at δ 129.7 similar to that (δ 118.7) of the X-ray-characterized²¹ vinyl complex Tp^{Me2}NbCl(CPh=CET₂)[=N-P(*i*-Pr)₂]. We have also attempted the synthesis of the known⁸ oxo complex Tp^{Me2}NbCl₂(O) starting from **1**, Zn, and propene oxide. However, the only oxo compound that we have been able to isolate was the known dimer [Tp^{Me2}Nb(O)Cl](μ-O).¹³ These results show that a reductive strategy leading to a Tp^{Me2}NbCl₂(L) complex from a niobium(IV) precursor Tp^{Me2}NbCl₃ is particularly efficient when L is an alkyne or an imido group and that a more intricate reaction course leads only to a dimer when an oxo complex was sought.

α-C-H Agostic Ethyl Complexes and Their Attempted Rearrangement. Among the interesting properties of Tp^{Me2} in Tp^{Me2}NbCl(alkyl)(alkyne) complexes are its directing properties that drive a bulky substituent on the alkyl in a wedge between two pyrazolyl rings. These directing effects lead to the discovery of unique examples of equilibria between α- and β-CH agostic rotamers in secondary alkyl complexes.²² C-C bond metathesis occurring via a reversible migratory insertion of the coordinated alkyne into the Nb-C was observed when an α-CH agostic linear alkyl was present. Only ≡C-C, not ≡C-Ph, was metathesized.²¹ This is summarized in Scheme 5. The Nb-CH₃ bond dissociation energy (BDE) is sufficiently high to drive the metathesis reaction all the way to the methyl complex. A Nb-*n*-propyl bond equilibrates with a Nb-ethyl bond since the ≡C-C BDE is not expected to vary to a large extent between ≡C-CH₂CH₃ and ≡C-CH₂CH₂CH₃. That the phenyl does not migrate indicates either an α-CH agostic interaction that sta-

Scheme 5



Scheme 6



R = CH₂Ph, Ph, 4-C₆H₄Me

bilizes the Nb-ethyl bond with respect to a Nb-Ph bond and/or a high barrier for the migration of the phenyl ring to the niobium. In the case of terminal alkyne complexes Tp^{Me2}NbCl(alkyl)(HC≡CR), it seemed of interest to probe the migratory aptitudes of H versus R. Kinetically, it is well known that migratory aptitudes of H are higher than those of R.²³ Thermodynamically, transition metal alkyl (M-C) BDEs are weaker than M-H BDEs, although this trend is not pronounced for early transition metal d⁰ systems.²⁴ We thus sought to compare the bonding energetics of the systems consisting of a terminal alkyne bound to an α-agostic ethyl niobium Tp^{Me2}Nb(μ-H-CHCH₃)Cl moiety as described in Scheme 6. This would offer the opportunity to further test the reactivity of well-defined α-C-H-agostic ethyl complexes and intramolecularly compare relative M-H, M-C and C-H, C-R BDEs. Depending on the relative BDEs, migration of the Nb(μ-H-CHCH₃) group to the

(21) Etienne, M.; Mathieu, R.; Donnadiou, B. *J. Am. Chem. Soc.* **1997**, *119*, 3218–3228.

(22) Jaffart, J.; Etienne, M.; Maseras, F.; McGrady, J. E.; Eisenstein, O. *J. Am. Chem. Soc.* **2001**, *123*, 6000–6013.

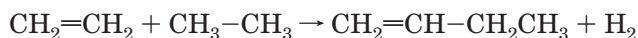
(23) (a) Brookhart, M.; Hauptman, E.; Lincoln, D. M. *J. Am. Chem. Soc.* **1992**, *114*, 10394–10401. (b) Burger, B. J.; Santarsiero, B. D.; Trimmer, M. S.; Bercaw, J. E. *J. Am. Chem. Soc.* **1988**, *110*, 3134–3146. (c) Jordan, R. F. *Adv. Organomet. Chem.* **1991**, *31*, 325–387.

(24) (a) *Bonding energetics in organometallic compounds*; Marks, T. J., Ed.; ACS Symposium Series 428; American Chemical Society: Washington DC, 1990. (b) Thompson, M. E.; Baxter, S. M.; Bulls, A. R.; Berger, B. J.; Nolan, M. C.; Santarsiero, B. D.; Schaefer, W. P.; Bercaw, J. E. *J. Am. Chem. Soc.* **1987**, *109*, 203–219. (c) Schaller, C. P.; Cummins, C. C.; Wolczanski, P. T. *J. Am. Chem. Soc.* **1996**, *118*, 591–611. (d) Bryndza, H. E.; Fong, L. K.; Paciello, R. A.; Tan, W.; Bercaw, J. E. *J. Am. Chem. Soc.* **1987**, *109*, 1444–1456. (e) Jones, W. D.; Hessell, E. T. *J. Am. Chem. Soc.* **1993**, *115*, 554–562. (f) Clot, E.; Besora, M.; Maseras, F.; Mégret, C.; Eisenstein, O.; Oelckers, B.; Perutz, R. N. *Chem. Commun.* **2003**, 490–491.

alkyne followed by H migration to Nb might indeed be favorable (Scheme 6). Assuming an sp^2 -type hybridization for the Nb-bound carbons of the alkyne, the reaction enthalpy for the reaction in Scheme 6 is then

$$\Delta_r H^\circ(6) = [D(\text{Csp}^2\text{-H}) + D(\text{Nb-CH}_2\text{CH}_3)] - [D(\text{Csp}^2\text{-CH}_2\text{CH}_3) + D(\text{Nb-H})]$$

For an estimation of $D(\text{Csp}^2\text{-CH}_2\text{CH}_3)$ and $D(\text{Csp}^2\text{-H})$ in these complexes, one can rely on $D(\text{Csp}^2\text{-CH}_2\text{-CH}_3)$ for 1-butene and compare it with $D(\text{Csp}^2\text{-H})$ for ethene, and it thus uses the reaction



for which $\Delta_r H^\circ = \Delta_f H^\circ(\text{CH}_2\text{CH-CH}_2\text{CH}_3) - \Delta_f H^\circ(\text{C}_2\text{H}_6) - \Delta_f H^\circ(\text{C}_2\text{H}_4) = D(\text{C}_2\text{H}_5\text{-H}) + D(\text{C}_2\text{H}_3\text{-H}) - D(\text{H}_2) - D(\text{CH}_2\text{CH-CH}_2\text{CH}_3)$.

With values taken from literature,²⁵ $D(\text{CH}_2\text{CH-CH}_2\text{-CH}_3) = -\Delta_f H^\circ(\text{CH}_2\text{CH-CH}_2\text{CH}_3) + \Delta_f H^\circ(\text{C}_2\text{H}_6) + \Delta_f H^\circ(\text{C}_2\text{H}_4) + D(\text{C}_2\text{H}_5\text{-H}) + D(\text{C}_2\text{H}_3\text{-H}) - D(\text{H}_2) = 0.13 + 84.7 - 52.3 + 419 + 444 - 436 = 460 \text{ kJ}\cdot\text{mol}^{-1}$. This value is higher than $D(\text{C}_2\text{H}_3\text{-H})$ for ethene and $D(\text{CH}_2\text{-CH-CH}_2\text{CH}_3) - D(\text{C}_2\text{H}_3\text{-H}) \approx 14 \text{ kJ}\cdot\text{mol}^{-1}$.

As a guideline, transition metal M-H bonds are generally stronger than M-R bonds. They are of comparable magnitude at d^0 metal centers when $R = \text{CH}_3$, which yields the strongest M-*n*-alkyl bond. M-CH₂-CH₃ bonds are usually ca. $15 \text{ kJ}\cdot\text{mol}^{-1}$ weaker than M-CH₃ bonds.²⁶ For a formally d^2 Nb(III) center in Cp₂-Nb(CO)X (X = H, CH₃), photoelectron spectra yielded $D(\text{Nb-H}) - D(\text{Nb-CH}_3) \geq 50 \text{ kJ}\cdot\text{mol}^{-1}$, which translates to $D(\text{Nb-H}) - D(\text{Nb-CH}_2\text{CH}_3) \geq 65 \text{ kJ}\cdot\text{mol}^{-1}$.²⁷ Considering that the strength of the α -C-H agostic interaction in Tp^{Me2}Nb(μ -H-CHCH₃)Cl(alkyne) is not known and that the bonding in these complexes can be described with a strong Nb(V), d^0 , contribution, the $D(\text{Nb-H}) - D(\text{Nb-CH}_2\text{CH}_3) = 65 \text{ kJ}\cdot\text{mol}^{-1}$ difference is certainly an upper limit. However, it is unlikely that it shrinks to ca. $10\text{--}15 \text{ kJ}\cdot\text{mol}^{-1}$, the difference observed for $D(\text{Zr-H}) - D(\text{Zr-CH}_2\text{CH}_3)$ in tris(amido)Zr(IV) complexes.^{24c} Even so, the overall analysis suggests that the reaction in Scheme 6 would be exothermic ($\Delta_r H^\circ(6) < 0$) and thus favorable since entropy effects are likely to cancel out. Note however that despite repeated attempts we have never been able to synthesize hydride complexes based on Tp^{Me2}NbCl₂(alkyne).

α -C-H agostic ethyl complexes Tp^{Me2}Nb(μ -H-CHCH₃)Cl(HC≡CR) (**4-R**) (**R** = **Ph**, **C₆H₄-4-Me**, **CH₂Ph**) were prepared from **2-R** according to our previously described procedure.²¹ Key NMR features for the α -C-H agostic ethyl interaction include a shielded α -CHH proton (for **4-CH₂Ph**, δ 0.29, dq) and its deshielded α -CHH diastereotopic counterpart (δ 4.01, dq) with a large chemical shift difference, and in the ¹³C NMR spectra a NbC α

appearing as a deshielded doublet of doublets with one reduced and one augmented ¹J_{CH} (for **4-CH₂Ph**, δ 88.3, ¹J_{CH} 108, 132 Hz). These data are similar to those of other Nb and Ta ethyl complexes^{6,21} and to those of related Mo and W α -C-H agostic alkyl complexes.²⁸ Thermolyses of complexes **4-R** were conducted in benzene-*d*₆ at 323 K and followed by ¹H and ¹³C NMR spectroscopy. In complete contrast to the case of Tp^{Me2}-NbCl(μ -H-CHCH₃)(PhC≡CR),²¹ disappearance of **4-R** was deceptively accompanied by large amounts of ill-defined decomposition products. The formation of hydride complexes with rearranged alkynes according to Scheme 6 could not be unambiguously established. However, the following observations suggest that these rearrangements might have taken place. Significant changes in the ¹H NMR spectra include (i) the appearance of slightly broad singlets in the δ 16.5–17.2 region, generally two of unequal intensity, and (ii) the appearance of signals in the δ 4.4 and 4.0 regions in the form of quartets (q, *J* 7.5 Hz) and doublets of quartets (qd, *J* 7.5, 12.0 Hz), respectively. For (ii), the signals are characteristic of a coordinated (4e)-alkyne RC≡CCH₂-CH₃ within a symmetrical complex⁵ or within an asymmetric complex,²¹ respectively. In some cases, especially that of **4-C₆H₄-4-Me**, the symmetrical complex is by far the most abundant species. Associated with the methylene quartet are its accompanying triplet (δ 1.15), an AB type spectrum attributed to the aryl protons of C₆H₄-4-Me at δ 6.73 and 6.69 (*J* 6 Hz), and typical Tp^{Me2} methine (1:2 intensity pattern) and methyl (3:3:6:6 intensity pattern) signals. ¹³C NMR spectra confirm the disappearance of **3-R** and the formation of quaternary (4e)-alkyne carbons in the δ 200–260 region. These data clearly suggest that Tp^{Me2}NbCl₂(CH₃CH₂C≡CR) has been formed from **4-R**. The formation of this coordinated alkyne clearly indicates that the rearrangement has occurred; that is, at some stage the migratory insertion of HC≡CR into the Nb(CH₂CH₃) bond has taken place, followed by formation of an unstable NbH species with a coordinated CH₃CH₂C≡CR.²¹ This is also supported by the presence of an unsymmetrical species that contains this rearranged alkyne ((ii) above), i.e., Tp^{Me2}-NbCl(X)(CH₃CH₂C≡CR). Importantly, the observation of deshielded *quaternary* carbon resonances indicate that no putative niobium ethylidene complex of the type Tp^{Me2}Nb(=CHCH₃)(L)(RC≡CR') has been formed via an α -elimination pathway, a species that could have shown the ¹H NMR signals in the δ 16 region ((i) above). Now, would it be possible that these deshielded signals are those of NbH species? Clearly, these signals are not pyrazole-NH protons that might have been formed by decomposition of Tp^{Me2} since these protons exhibit much broader signals in the δ 11 region in benzene-*d*₆. Formally Nb(III), d^2 complexes with an 18e count exhibit hydride chemical shifts with various chemical shifts, usually negative (Cp₂NbH(C₂H₃Ph),^{23b} δ -2.40, -2.89; Cp₂NbH(PhC≡CPh),²⁹ δ -0.23). For true d^0 complexes, the hydride is much more deshielded. In a series of imidotantalum(V) complexes that are similar

(25) (a) *Physical chemistry*, 6th ed.; Atkins, P. W., Ed.; Oxford University Press: Oxford, 1998. (b) *CRC Handbook of Chemistry and Physics*; Weast, R. C., Astle, M. J., Beyer, W. H., Eds.; CRC Press Inc.: Boca Raton, FL, 1988.

(26) Dias, A. R.; Diogo, H. P.; Griller, D.; Minas de Piedade, M. E.; Martinho Simoes, J. A. In *Bonding energetics in organometallic compounds*; Marks, T. J., Ed.; ACS Symposium Series 428; American Chemical Society: Washington DC, 1990; pp 205–217, and references therein.

(27) Lichtenberger, D. L.; Darsey, G. P.; Kellog, G. E.; Sanner, R. D.; Young, V. G., Jr.; Clark, J. R. *J. Am. Chem. Soc.* **1989**, *111*, 5019–5028.

(28) (a) Bau, R.; Mason, S. A.; Patrick, B. O.; Adams, C. S.; Sharp, W. B.; Legzdins, P. *Organometallics* **2001**, *20*, 4492–4501. (b) Wada, K.; Pamplin, C. B.; Legzdins, P.; Patrick, B. O.; Tsyba, I.; Bau, R. *J. Am. Chem. Soc.* **2003**, *125*, 7035–7048.

(29) Yasuda, H.; Yamamoto, H.; Arai, T.; Nakamura, A.; Chen, J.; Kai, Y.; Kasai, N. *Organometallics* **1991**, *10*, 4058–4066.

to our Nb complexes, i.e., (C₅Me₅)TaH(X)=NAr (Ar = 2,6-(2,4,6-C₆H₂Me₃)₂C₆H₃ and related aryl groups), chemical shifts as high as δ 15.28 (X = Cl) and δ 15.20 (X = OTf) have been observed.^{30a} In (C₅Me₅)TaH(X)[PhSiH₂-NPhSiMe₃]NSiMe₃, the hydride resonates at δ 17.15 (X = Me) and δ 20.44 (X = Cl).^{30b} Overall, although we have as yet no definitive proof of hydride complexes, NMR data strongly suggest that the sought rearrangement in Scheme 6 has taken place. However no reliable thermodynamic and kinetic data can be extracted.

Summary. In this paper we have disclosed a straightforward, efficient synthesis of terminal alkyne complexes of the type Tp^{Me}NbCl₂(HC≡CR) that uses Zn reduction of Tp^{Me}NbCl₃ in the presence of the desired alkyne. The overall alkyne orientation with respect to Tp^{Me}NbCl₂ has been discussed in terms of steric interactions. For trifluoropropyne, intramolecular H...F bridges contribute to the cocrystallization of different alkyne rotamers. α -C-H alkyl complexes are also available. Their thermolysis has suggested that reversible migratory insertion might yield hydride complexes, although the instability of these complexes has precluded a detailed investigation of the reaction course.

Experimental Section

General Procedures. All experiments were carried out under a dry dinitrogen atmosphere using either Schlenk tube or glovebox techniques. THF and diethyl ether were obtained after refluxing purple solutions of Na/benzophenone under dinitrogen. Toluene, *n*-hexane, pentane, 1,4-dioxane, and dichloromethane were dried by refluxing over CaH₂ under dinitrogen. Deuterated NMR solvents were dried over molecular sieves, degassed by freeze-pump-thaw cycles, and stored under dinitrogen. ¹H and ¹³C NMR spectra were obtained on Bruker AM 250, DPX 300, AMX 400, or DRX 500 spectrometers, and ¹⁹F spectra (external reference CF₃CO₂H, chemical shifts versus CFCl₃ with δ (CF₃CO₂H) -77.0) were obtained on a Bruker AC 200. Only pertinent ¹J_{CH} are quoted in the ¹³C spectra. Due to the sometimes extreme complexity of the spectra and/or overlaps, several signals might not be observed. Elemental analyses were performed in the Analytical Service of our Laboratory. NbCl₄(thf)₂,³¹ Tp^{Me}NbCl₃ (**1**),¹⁰ Tp^{Me}-SnClBu₂, and Tp^{Me}SnClBu₂^{11,12} were prepared according to published procedures. An improved synthesis of Tp^{Me}NbCl₃ is described below with that of Tp^{Me}SnClBu₂ (**1-CI**). Acetylene was generated by controlled hydrolysis of commercial sodium acetylide in xylene, passed through two cold traps (-25 °C, ethanol/liquid nitrogen baths) before being admitted in the Schlenk tube containing the appropriate reactants.

Tp^{Me}SnClBu₂ (1-CI). A solution of Tp^{Me}SnBu₂Cl (4.70 g, 8.32 × 10⁻³ mol) in 100 mL of toluene is added to a suspension of NbCl₄(THF)₂ (3.15 g, 8.32 mmol) in 150 mL of toluene, at room temperature. The resulting brownish slurry is stirred for 4 days in the dark. The solvent is evaporated to dryness, and 250 mL of dichloromethane is added. This mixture is stirred for 2 days to yield an orange powder, which is collected by filtration. The dark green solution is evaporated to half, and 100 mL of hexane is added to induce a new crystallization, which continues at -25 °C. The two solids are washed with two portions of 15 mL of diethyl ether and dried under vacuum (3.22 g, 6.49 mmol, 78%). Anal. Calcd for C₁₅H₁₉-BCl₆N₆Nb: C, 30.04; H, 3.19; N, 14.01. Found: C, 30.43; H,

2.97; N, 13.78. ESR (ν = 9.4797 GHz, 293 K, CH₂Cl₂): g = 1.94; A = 170 G (10 lines); (CH₂Cl₂/toluene glass, 100 K): g_1 = 1.909; A_1 = 260 G; g_2 = 1.940; A_2 = 124 G; g_3 = 1.926; A_3 = 126 G. IR (KBr, cm⁻¹): ν (B-H) 2567, ν (C-Cl) 860, ν (C≡N) 1527.

Tp^{Me}NbCl₂(PhC≡CH) (2-Ph). All Tp^{Me}NbCl₂(HC≡CR) complexes were prepared following the same general procedure that is described here in detail for Tp^{Me}NbCl₂(PhC≡CH) (**2-Ph**). PhC≡CH (0.12 g, 1.2 mmol) was added at room temperature to a stirred suspension of Tp^{Me}NbCl₃ (0.500 g, 1.00 mmol) in THF (50 mL) and granular zinc (30 mesh, 0.13 g, 2 mmol). The color of the solution gradually changed from orange to green and finally after about 1 h to dark purple. Stirring was maintained overnight. The volatiles were then removed under vacuum. Toluene (20 mL) was added and then stripped off. This process was repeated two times to remove traces of THF. The residue was extracted in toluene or dichloromethane (ca. 5 mL). Addition of pentane or hexane (10 mL) was followed by filtration through a pad of Celite. The extraction step was carried out several times. The clear dark red solution was then evaporated to dryness to obtain a red-purple microcrystalline powder, which was found pure enough for further chemistry (0.434 g, 0.77 mmol, 77%). Recrystallization from dichloromethane/pentane mixtures yielded an analytically pure sample of **2-Ph**. Anal. Calcd for C₂₃H₂₈BCl₂N₆Nb: C, 49.06; H, 5.01; N, 14.92. Found: C, 49.54; H, 5.40; N, 14.02. ¹H NMR (300 MHz, chloroform-*d*₁, 233 K): major rotamer δ 11.99 (s, 1H, HC≡C), 8.25, 7.75–7.64 (m, 5H, C₆H₅), 6.04, 5.98 (both s, 1:2H, Tp^{Me}CH), 2.75, 2.50, 2.47, 1.97 (all s, 3:3:6:6H, Tp^{Me}CH₃); minor rotamer δ 13.78 (s, 1H, HC≡C), 7.35 (m, 5H, C₆H₅), 5.98, 5.83 (both s, 1:2H, Tp^{Me}CH), 2.67, 2.54, 2.51, 1.70 (all s, 3: 6: 3: 6H, Tp^{Me}CH₃). ¹³C NMR (75.5 MHz, chloroform-*d*₁, 233 K): major rotamer δ 249.9, 218.7 (PhC≡CH, ¹J_{CH} 199 Hz), 153.9, 153.1, 145.5, 145.4 (Tp^{Me}CCH₃), 135.9, 134.7, 132.2, 129.5 (C₆H₅), 108.9, 108.6 (Tp^{Me}CH), 16.4, 13.9 (Tp^{Me}CH₃); minor rotamer δ 250.0, 221.0 (PhC≡C, HC≡C, ¹J_{CH} 205 Hz), 154.2, 153.5, 145.5, 145.2 (Tp^{Me}CCH₃), 135.9, 131.3, 129.7, 128.9 (C₆H₅), 109.1, 108.8 (Tp^{Me}CH), 16.6, 14.1 (Tp^{Me}CH₃); isomer ratio 3:1.

Tp^{Me}NbCl₂(CF₃C≡CH) (2-CF₃). ¹H NMR (200 MHz, benzene-*d*₆, 293 K): δ 11 (vbr, $W_{1/2}$ 100 Hz, 1H, HC≡C), 5.55, 5.34 (both s, 1:2H, Tp^{Me}CH), 2.81, 2.04, 1.93, 1.90 (all s, 3: 3: 6: 6H, Tp^{Me}CH₃). ¹⁹F{¹H} NMR (189 MHz, benzene-*d*₆, 293 K): δ 17.93. ¹H NMR (500 MHz, toluene-*d*₈, 193 K): major rotamer δ 9.80 (s, 1H, HC≡C), 5.42, 5.19 (both s, 1:2H, Tp^{Me}CH), 2.86, 2.13, 1.84, 1.78 (all s, 3:3:6:6H, respectively, Tp^{Me}CH₃); minor rotamer δ 12.24 (s, 1H, HC≡C), 5.39, 5.25 (both s, 1:2H, Tp^{Me}CH), 2.97, 2.09, 1.96, 1.69 (all s, 3:6:3:6H, Tp^{Me}CH₃). ¹³C NMR (125 MHz, toluene-*d*₈, 193 K): major rotamer δ 225.5 (q, ²J_{CH} 44 Hz, CF₃C≡C), 209.2 (HC≡C), 153.5, 152.25, 144.5, 144.2 (Tp^{Me}CCH₃), 108.2, 107.8 (Tp^{Me}CH), 15.4, 12.4, 12.3 (Tp^{Me}CH₃); minor rotamer δ 243.0 (HC≡C), 196.1 (q, ²J_{CH} 43 Hz, CF₃C≡C), 152.9, 144.2 (Tp^{Me}CCH₃), 127.1 (q, ²J_{CF} 271 Hz, CF₃), 107.7 (Tp^{Me}CH), 16.5, 15.9 (Tp^{Me}CH₃); isomer ratio 3.5:1.

Tp^{Me}SnCl₂(PhC≡CH) (2-CI-Ph). Anal. Calcd for C₂₃H₂₅-BCl₅N₆Nb: C, 41.45; H, 3.78; N, 12.61. Found: C, 41.80; H, 4.07; N, 12.23. ¹H NMR (300 MHz, toluene-*d*₈, 233 K): major rotamer δ 11.20 (s, 1H, HC≡C), 8.29, 7.34–7.20 (m, 5H, C₆H₅), 3.05, 2.15, 1.96, 1.77 (all s, 3:3:6:6H, Tp^{Me}CH₃); minor rotamer δ 13.42 (s, 1H, HC≡C), δ 7.09 (m, 5H, C₆H₅). ¹³C NMR (75.5 MHz, toluene-*d*₈, 233 K): major rotamer δ 249.0, 218.6 (d, ¹J_{CH} 196 Hz, PhC≡CH), 150.1, 149.3, 141.4, 141.3 (Tp^{Me}CCH₃), 134.9, 129.5, 128.8, 128.4 (C₆H₅), 111.1, 110.8 (Tp^{Me}CH), 14.30, 13.72, 10.75, 10.67 (Tp^{Me}CH₃); minor rotamer δ 250.0, 219.2 (PhC≡CH); isomer ratio 5:1.

Tp^{Me}NbCl₂(HC≡CC₆H₄-4-Me) (2-C₆H₄-4-Me). Anal. Calcd for C₂₄H₃₀BCl₂N₆Nb: C, 49.94; H, 5.24; N, 14.56. Found: C, 49.43; H, 5.25; N, 14.13. ¹H NMR (250 MHz, toluene-*d*₈, 193 K): major rotamer δ 11.30 (s, 1H, HC≡C), δ 8.35, 7.16 (both d, J 7.7 Hz, 2H each, C₆H₄), 5.55, 5.29 (both s, 1:2H,

(30) (a) Gavenonis, J.; Tilley, T. D. *Organometallics* **2004**, *23*, 31–43. (b) Gountchev, T. I.; Tilley, T. D. *J. Am. Chem. Soc.* **1997**, *119*, 12831–12841.

(31) Pedersen, S. F.; Hartung, J. B.; Roskamp, E. J.; Dragovitch, P. S. *Inorg. Synth.* **1992**, *29*, 119–123.

Table 4. X-ray Diffraction Analysis of Compounds 2-CH₂Ph and 2-CF₃

	2-CH ₂ Ph	2-CF ₃
Crystal Data		
chemical formula	C ₄₀ H ₃₀ BCl ₂ N ₆ Nb	C ₁₈ H ₂₃ BCl ₂ F ₃ N ₆ Nb,(H ₂ O) _{1/3}
cryst syst	triclinic	triclinic
space group	<i>P</i> 1	<i>P</i> 1
<i>a</i> (Å)	10.4566(8)	13.909(5)
<i>b</i> (Å)	11.1476(7)	16.844(5)
<i>c</i> (Å)	11.1476(7)	17.769(5)
α (deg)	74.971(5)	72.442(5)
β (deg)	85.341(5)	71.083(5)
γ (deg)	84.280(6)	70.172(5)
<i>V</i> (Å ³)	1338.72(15)	3618(2)
<i>Z</i>	2	6
μ (cm ⁻¹)	6.73	7.63
Data Collection		
diffractometer	Oxford Excalibur	STOE IPDS
radiation type	Mo Kα	Mo Kα
wavelength (Å)	0.71073 (graphite monoch.)	0.71073 (graphite monoch.)
temperature (K)	180(2)	180(2)
θ range (deg)	3.47–28.22	1.99–26.18
<i>h k l</i> range	–13 ≤ <i>h</i> ≤ 10 –14 ≤ <i>k</i> ≤ 14 –15 ≤ <i>l</i> ≤ 15	–17 ≤ <i>h</i> ≤ 17 –20 ≤ <i>k</i> ≤ 20 –22 ≤ <i>l</i> ≤ 22
no. of measd reflns	11 779	36 257
no. of indep reflns	6578	7257
merging <i>R</i> value	0.0294	0.050
Refinement		
absorption corr	empirical (DIFABS)	semiempirical (multiscan)
max. and min. transmn	0.92/0.85	0.95/0.90
refinement	<i>F</i> ² (full-matrix least-squares)	<i>F</i> (full-matrix least-squares)
no of reflns used	6578 [<i>I</i> > 2σ(<i>I</i>)]	7257 [<i>I</i> > 2σ(<i>I</i>)]
no of params used	416	847
final <i>R</i> ^a / <i>wR</i> ^{2b}	0.0299/0.0774	0.0437/0.0488
final <i>R</i> ^a / <i>wR</i> ^{2b} (all data)	0.0337/0.0798	
GOF (<i>S</i>) ^c	1.061	1.094

$$^a R = \sum(|F_o| - |F_c|)/\sum|F_o|. \quad ^b R_w = [\sum w(|F_o| - |F_c|)^2/\sum(|F_o|)^2]^{1/2}. \quad ^c \text{Goodness of fit} = [\sum(|F_o - F_c|)^2/(N_{\text{obs}} - N_{\text{parameters}})]^{1/2}.$$

cycles of refinement a weighting scheme was used, where weights are calculated from the following formula: $w = 1/[\sigma^2(F_o^2) + (aP)^2 + bP]$, where $P = (F_o^2 + 2F_c^2)/3$. For **2-CF₃**, the asymmetric unit contained three H₂₃BCl₂F₃N₆Nb molecules and one disordered water molecule. All non-hydrogen atoms excluding the water molecules were refined anisotropically. Hydrogen atoms were introduced in calculated positions in the last refinements and were allocated an overall refinable isotropic thermal parameter. A weighting scheme of the form $w = w'[1 - (||F_o| - |F_c||/6\sigma(F_o))^2]$ with $w' = 1/\sum_r A_r T_r(X)$ with coefficients 3.15, –1.04, and 2.62 for a Chebychev series for

which $X = F_o/F_c(\text{max})$ was used. Drawings of molecules were performed with the program ORTEP3³⁷ with 30% probability displacement ellipsoids for non-hydrogen atoms.

Supporting Information Available: Cif files for the X-ray characterization of **2-CH₂Ph** and **2-CF₃**. This material is available free of charge via the Internet at <http://pubs.acs.org>.

OM050423F

(37) ORTEP3 for Windows. Farrugia, L. J. *J. Appl. Crystallogr.* **1997**, *30*, 565.